AN ABSTRACT OF THE THESIS OF

William Henderson Peek for the Master of Science

in Electrical and Electronics Engineering presented on *May 7, 1968*

Title: A Flux-Coupled Current Measuring System with a

Bandwidth from D.C. to Fifty Megahertz

Abstract approved: ███████████████████████
Leland C. Jensen

An instrument which measures current from D.C. to 50 megahertz by clipping a transformer core around a current carrying conductor is discussed. A Hall device, which is installed in the core cross-section, detects the flux in the core. This Hall device in conjunction with an amplifier is used to null the low frequency components of flux generated in the core by the current in the conductor. A multi-turn secondary winding performs the same type of operation at high frequencies. The current generated by these two methods, which is proportional to the input current, is amplified and measured with an oscilloscope or other suitable instrument. The mode of operation and the characteristics of the system are analyzed, with emphasis upon the midfrequency range. Results of measurements from an operating system are given and correlation to the model is shown.

A Flux-Coupled Current Measuring System
with a Bandwidth from
D.C. to Fifty Megahertz

by

William Henderson Peek

A THESIS

submitted to

Oregon State University

in partial fulfillment of
the requirements for the
degree of
Master of Science
June 1968

APPROVED:

Professor of Electrical and Electronics Engineering
in charge of major

Head of Department of Electrical and Electronics Engineering

Dean of Graduate School

Date Thesis is presented ....*May 7, 1968*..........

Typed by Virginia McElfresh for William H. Peek

ACKNOWLEDGEMENTS

TABLE OF CONTENTS

LIST OF FIGURES

A Flux-Coupled Current Measuring System with a

Bandwidth from D.C. to Fifty Megahertz

I.   INTRODUCTION

The development and application of semiconductor devices during
the past ten years has been very rapid. Many of these semiconductor
devices are current sensitive devices or are operated in the current
dependent mode. This has created a need for a current measuring
device. This need includes waveform analysis over a broad frequency
range as well as amplitude measurements.

This thesis discusses a current probe which will partially
satisfy this instrumentation need. The current measuring device has
a dynamic range from one milliamp to ten amps, a frequency response
from D.C. to 50 MHz, and an output suitable for use with an oscillo-
scope so waveforms can be easily analyzed. It is a clip-on type
probe which eliminates the need to open the circuit under test.

Several devices are available for current detection such as:
a series resistor; a standard turns-ratio transformer; Hall devices;
magneto-strictive devices; cross-field modulation; and second-
harmonic detection of transformer core saturation. (5:665)

A series resistor may make a very good current detector if it
is already in the circuit, but in general, has some disadvantages.
One disadvantage is that the circuit must be broken to insert the
resistor. Another disadvantage is that the voltage across the
resistor must be measured, usually differentially, which adds unde-
sirable stray impedance to the circuit under test.

The probe should make no physical connection to the circuit and add a minimum amount of stray impedance to the circuit. A system of flux detection involving flux-coupling in a high permeability material is one method of accomplishing this end.

Hall devices and magneto-strictive devices are basically flux detectors. The Hall device has a lower sensitivity to noise ratio than some magneto-strictive devices, but magneto-strictive devices do not retain polarity integrity. That is, resistance increases regardless of the polarity of the flux density passing through the device. Hall and magneto-strictive devices have bandwidth limitations associated with their internal resistance and capacitance to their surroundings.

Standard transformers operate on flux linkages and have been used to measure current for many years. They have good high frequency response but are not capable of detecting direct current.

The cross-field modulation and second-harmonic detection methods have practical bandwidth limits which are five to ten times below their modulating frequencies. They have the further disadvantage that the modulating signal in the core, if not perfectly balanced, can be generated into the input. These methods are capable of less noise and therefore more sensitivity than other detection methods discussed here.

II.   THE SYSTEM

A system composed of a Hall device in combination with a trans-
former is discussed in this thesis. The combination of the transfor-
mer and Hall device has two advantages over complete reliance upon
the Hall device. One advantage is that the upper frequency response
limit is the same as for a standard transformer, in this case about
50 MHz. The second advantage is a marked reduction in noise from
the Hall device by limiting its bandwidth. Figure 2.1 schematically
illustrates the system to be discussed.
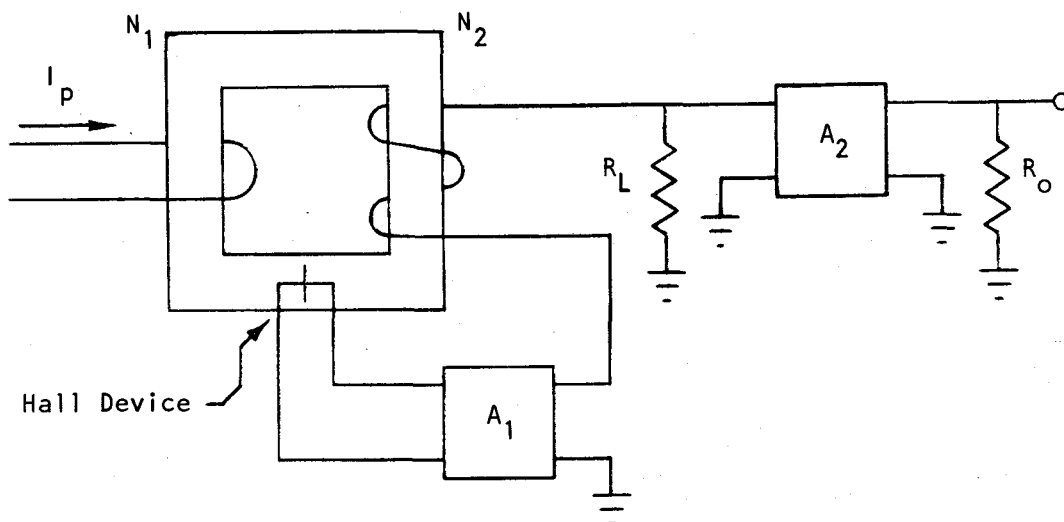
Figure 2.1   A Schematic Illustration of the Current
Measuring System

For low frequencies, the Hall device in the system detects the
net flux in the core and produces a low level voltage for amplifier
A_1. Amplifier A_1 is a high gain amplifier with a low output imped-
ance. It amplifies the Hall device voltage and causes a current to
flow through the secondary turns and the load resistor R_L. The MMF
created in the core by the secondary current cancels most of the

MMF created by the primary current. The core is therefore a MMF summing point at low frequencies in which the null flux is detected by the Hall device.

At high frequencies the Hall device is not capable of providing a signal for amplifier A_1 and the system operates as a normal transformer. The flux in the core links the secondary turns and creates a voltage proportional to the rate of change of flux. This voltage causes a current to flow from the output of amplifier A_1, through the secondary turns and through R_L. At high frequencies the MMF created in the core by the secondary current cancels most of the MMF created by the primary current. The core is again a MMF summing point in which the rate of change of flux is now detected by the secondary winding. The voltage, proportional to the secondary current, across R_L is amplified by amplifier A_2 to a suitable level for use with a general purpose oscilloscope. The system under discussion has a secondary to primary turns-ratio of 50:1 and a load resistor R_L of 50 ohms. The voltage gain of amplifier A_2 is 50 and the output resistance R_o is 50 ohms. This results in an overall current to voltage transfer of 50 millivolts per milliamp.

A major portion of this thesis will discuss, in detail, the operation of the system in the midfrequency or crossover-frequency region.

III.   HALL DEVICE OPERATION

Core Construction

Figure 3.1 shows the physical arrangement of the Hall device
and the high permeability core material. The core consists of three
pieces known as the "I" bar, the "L" bar and the "closer" bar.
During the construction of the assembly, the Hall element is deposited
upon the "I" bar and leads are attached. An end of the "L" bar is
tapered to fit within the leads of the Hall device. The two pieces
are glued together with epoxy. The 50 secondary turns, not shown in
Figure 3.1, are then wound around the legs of the "L" and "I" bars.
The resulting assembly and the "closer" are then encased in a plastic
body. The plastic body allows the "closer" to be removed and replaced
easily so a primary wire can be placed on the opening without breaking
the electrical circuit.

The Hall Device Voltage

The Hall effect voltage in a Hall device is

$$E_{he} = \frac{R_h (\vec{I}_h \times \vec{B})}{T_h}$$

(3.1)

where E_{he} is the Hall effect voltage in volts, R_h is the Hall coeffi-
cient in volt-meter^3 / ampere-Weber, B is magnetic flux density in
Webers / meter^2, I_h is the Hall current in amperes, and where T_h
is the thickness of the Hall device in meters. (8:395) When the
Hall device is sandwiched in the core as shown in Figure 3.1, a
condition of normalcy exists between Hall voltage, Hall current and

6

FIGURE 3.1

Core Assembly
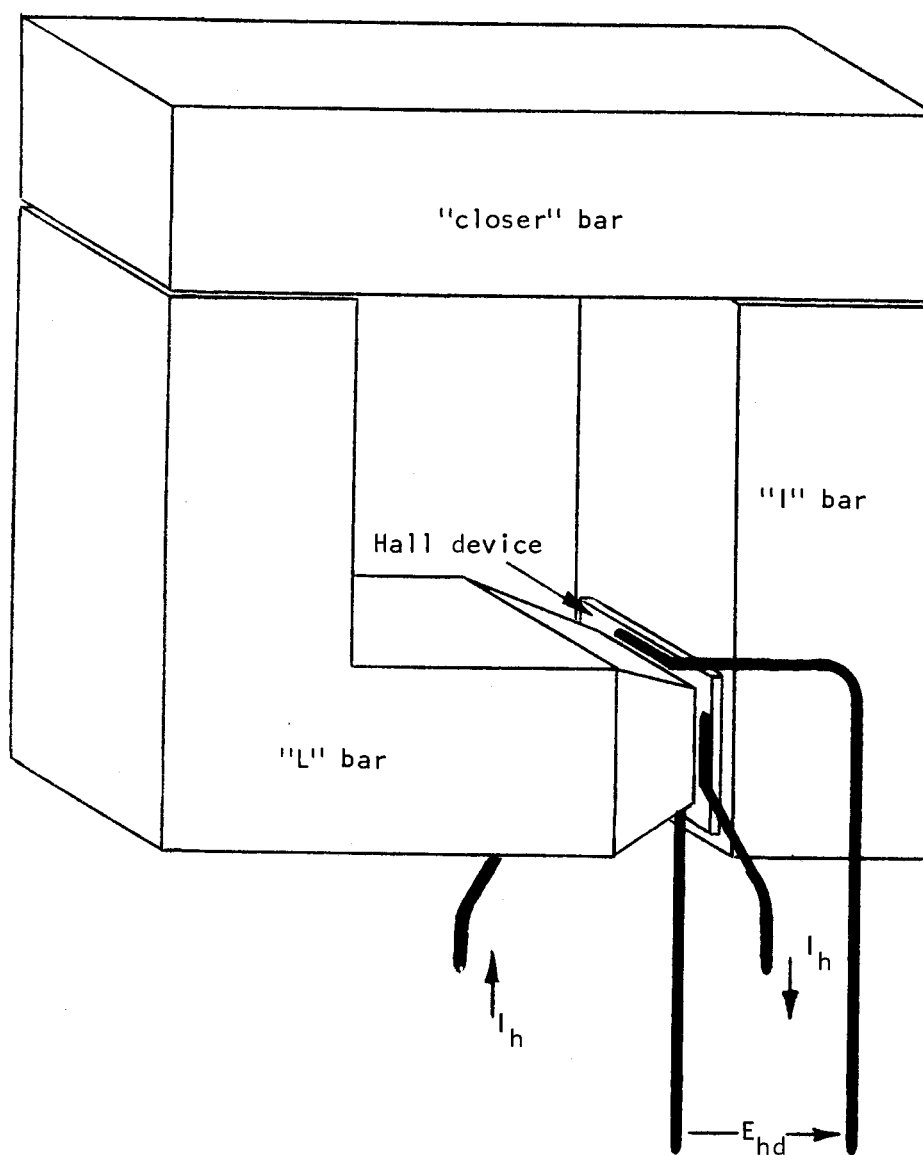
flux density and

$$E_{he} = \frac{R_h B \, I_h}{T_h} \qquad (3.2)$$

The "L" bar is tapered to conform to the active area of the Hall

element so

$$E_{he} = \frac{R_h I_h}{T_h} \frac{\Phi}{A_h} \qquad (3.3)$$

where magnetic flux density is equal to the flux per unit area

and Φ is the flux in Webers passing through the Hall device and A_h

is the area of the Hall element in meters^2.

A second Hall device output voltage is caused by the rate of

change of the flux linked by the output leads. The output leads are

geometrically centered on the Hall device so the leads link only one-

half of the flux in the core. The resulting voltage is

$$E_n = N_h \frac{d\frac{\Phi}{2}}{dT} = \frac{N_h}{2} \frac{d\Phi}{dT} \qquad (3.4)$$

where N_h is the number of turns of the Hall element output leads and

is equal to one, Φ is the net flux in the core and T is the variable

time. The Laplace transform of Equation 3.4 yields

$$E_n(s) = \frac{N_h}{2} S \, \Phi(s) \qquad (3.5)$$

where S is the Laplace variable and is equal to $\frac{d}{dT}$ when initial con-

ditions are zero and $\Phi(s)$ is the net flux in the core in terms of S.

(6:147) The $\frac{N_h}{2}$ term in Equation 3.5 leads to the term ½ turn voltage"

as the description of E_n. The total Hall device output voltage then

is the sum of the ½ turn voltage and the Hall effect voltage

expressed as

$$E_{hd}(s) = E_{he}(s) + E_n(s) = \frac{\Phi R_h I_h}{T_h A_h} \left(1 + \frac{N_h A_h T_h}{2 R_h I_h} S \right) \qquad (3.6)$$

where $E_{hd}(s)$ is the total Hall device output voltage as a function

of S, $E_{he}(s)$ is the Hall effect voltage of the Hall device as a

funtion of S, and $E_n(s)$ is the ½ turn voltage of the Hall device as

a function of S. A plot of measured Hall device voltage versus

frequency is shown in Figure 3.2.

Reluctance and Air Gaps

The conversion from ampere-turns to flux is important and is

related by the magnetic circuit relationship

$$\Phi = \frac{N I}{R} \qquad (3.7)$$

where Φ is the circuit flux in Webers, the product of N and I is the

magnetic potential in ampere-turns, and R is the reluctance of the

flux path length in ampere-turns / Weber. (10:36)

Air gaps are very critical in their effect upon the reluctance

of the flux path. Figure 3.3 is a plot of reluctance versus air gap

for the core assembly. The total air gap of the core assembly is

approximately 1.3×10^{-3} inches. This air gap consists of the thick-

ness of the Hall device, the effect of the tapered "L" bar at the Hall

device and two air gaps associated with the core "closer" as shown in

Figure 3.1.

Reluctance can be equated to inductance and turns as shown in

Appendix II where

Figure 3.2
Frequency Response of the Hall Device Voltage
with I_h = 18ma and I_p = 80ma.

Hall Device Voltage, mv

100

10

1

1k   10k   100k   1M   10M

Frequency, Hz

Figure 3.3
Reluctance versus Air Gap
in the Core Assembly

Reluctance, $\dfrac{\text{ampere-turns}}{\text{Weber}}$

Air Gap, microinches
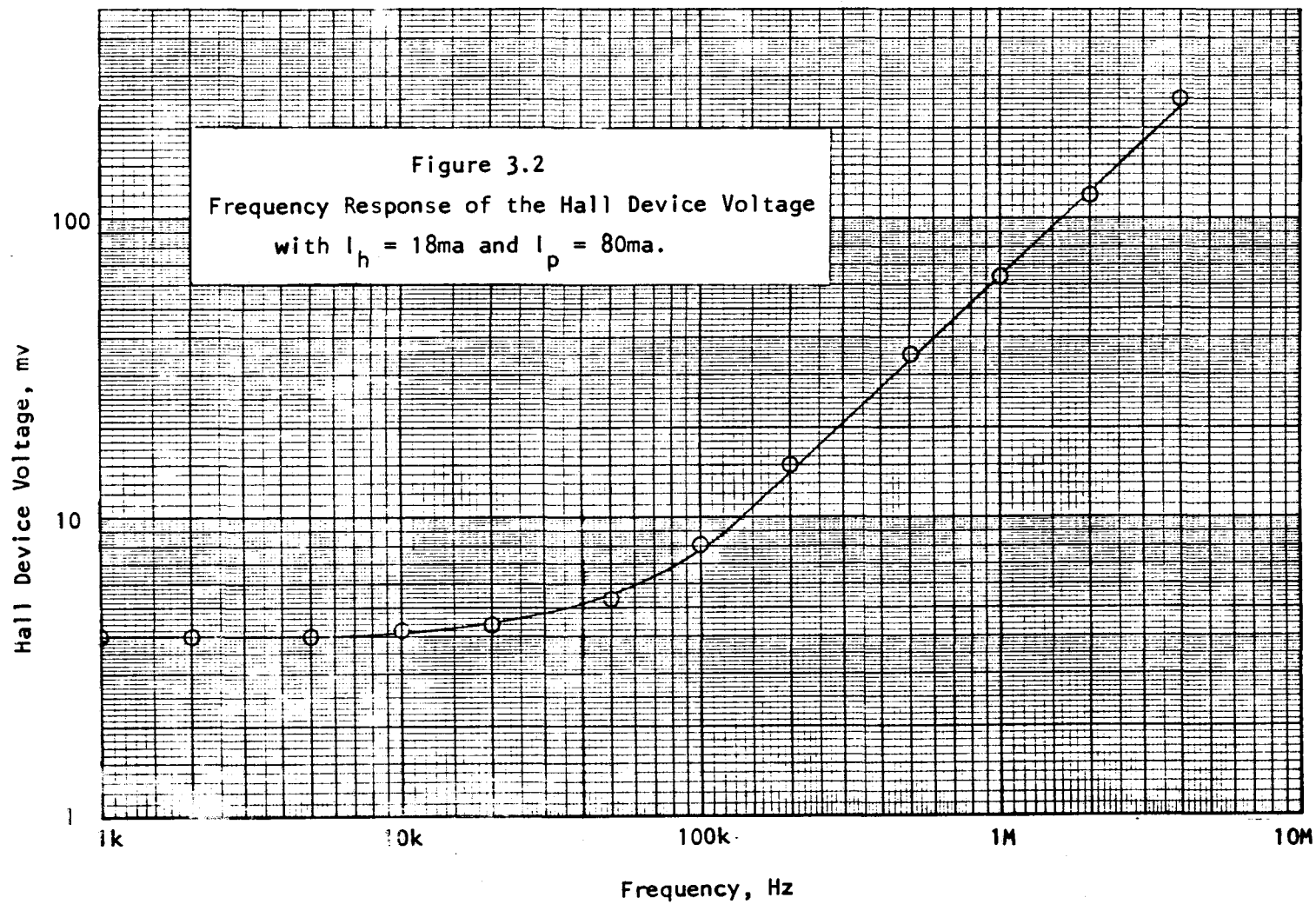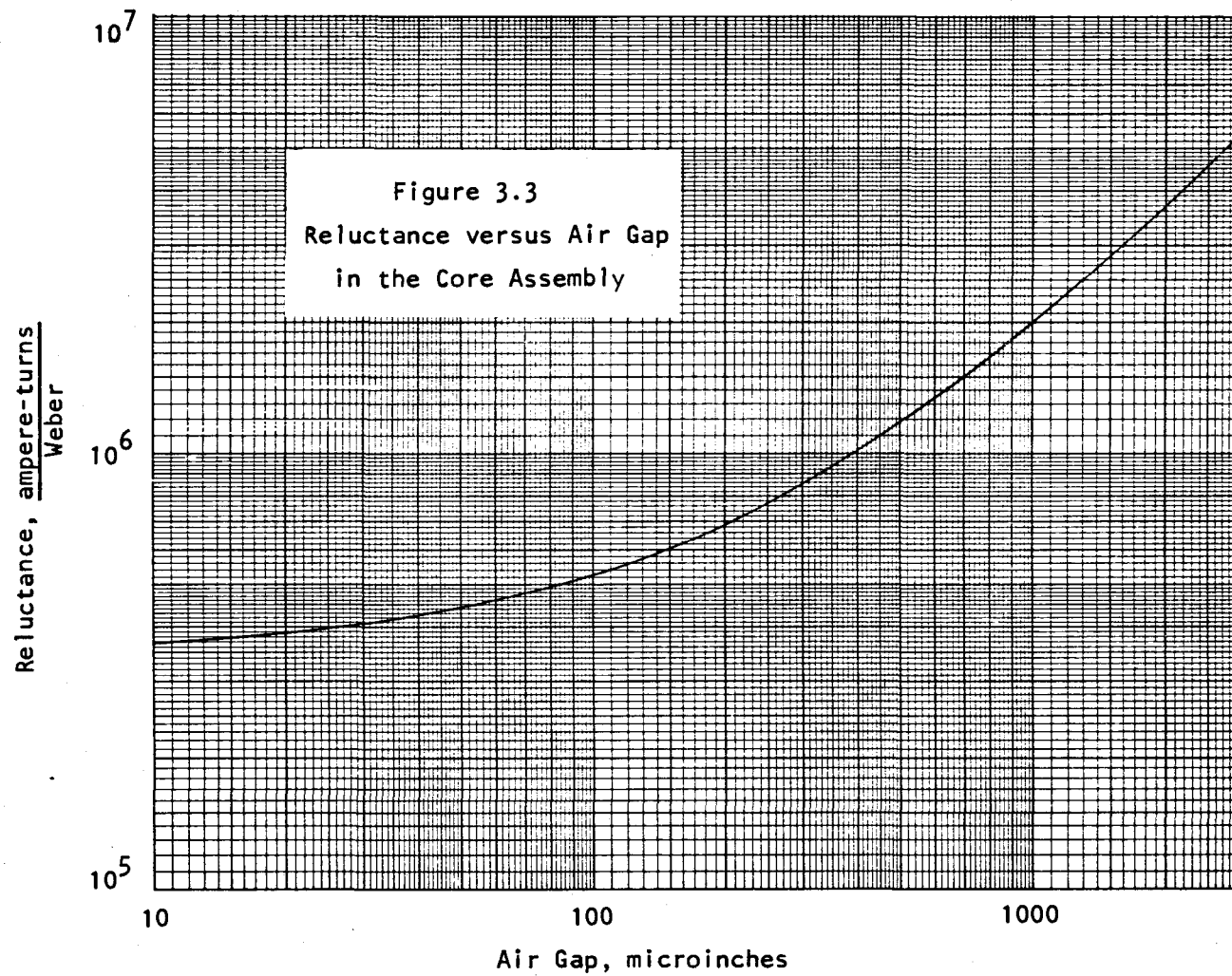
$$R = \frac{N_s^2}{L_s} \tag{3.8}$$

where N_s is the turns of the secondary winding, L_s is the inductance of the secondary winding, and R is the reluctance of the flux path. (3:3-34) The secondary winding of this system consists of 50 turns. From Figure 3.3 the reluctance of the core which has an effective air gap of 1.3×10^{-3} inches is 2.5×10^6 ampere-turns per Weber. Using Equation 3.8 to calculate the inductance of the secondary winding results in

$$L_s = \frac{N_s^2}{R} = \frac{2500}{2.5 \times 10^6} \approx 1 \times 10^{-3} \text{ Henrys.} \tag{3.9}$$

IV.   TRANSFORMER ANALYSIS

The Model

Figure 4.1 shows the transformer model and the sign convention used for this analysis.   In the model the voltage generator E_s
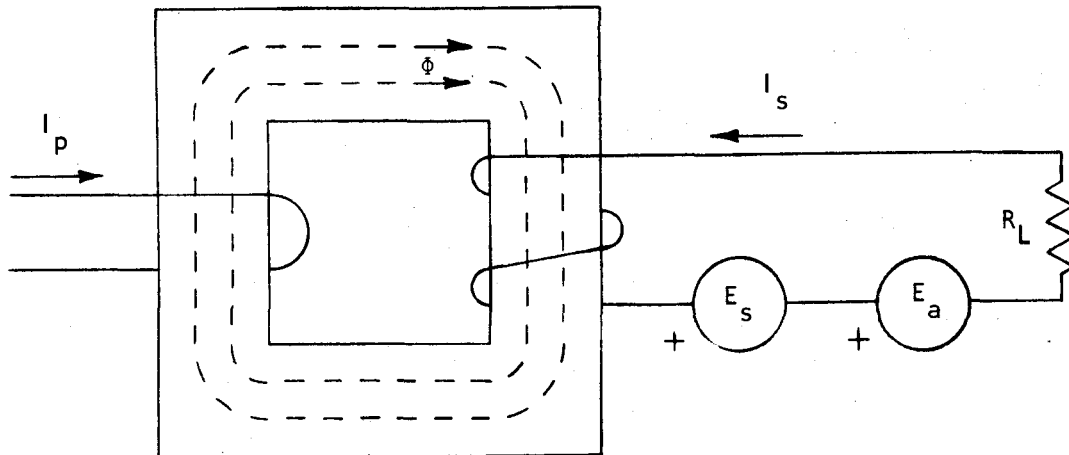
Figure 4.1.   The Transformer Model

represents the voltage developed across the transformer secondary winding.   The voltage generator E_a represents the output voltage of amplifier A_1 which amplifies the Hall voltage as shown in Figure 2.1.

Some assumptions are made about the physical transformer in order to generate this model.   One is that there is no leakage flux; all flux generated by either winding couples the other winding. Another assumption is that the total reluctance of the flux path is constant with frequency and magnitude of flux.   Other assumptions are that there are no other stray components of resistance, capacitance or inductance in the system.

The transformer model can be described as a feedback system shown as a diagram in 4.2   In the block diagram the product of the
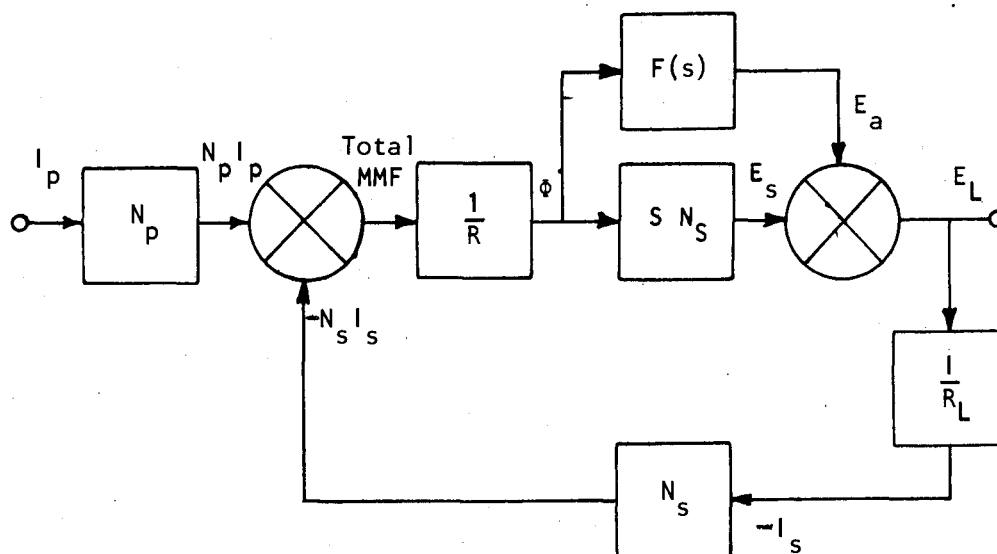
Figure 4.2 Block Diagram of the Transformer

input current I_p and the primary turns N_s produces a primary magnetic

potential along the transformer core. The product of the secondary

current I_s and secondary turns N_s produces another magnetic poten-

tial along the core. These two magnetic potentials are added in the

core and in the first summing element. The result is the total

magnetic potential around the transformer core. This total magnetic

potential is then divided by the reluctance of the core R to produce

the net core flux Φ which is the input to the two amplifying blocks.

One block F(s) represents the transfer from flux to voltage accom-

plished by the Hall device and amplifier A_1. The second block SN_s

represents the transfer from the rate of change of the flux to the

voltage across the secondary winding. The output of these two gain

blocks are summed in the secondary loop to produce the output voltage

E_L. The output voltage then causes a secondary current I_s to flow

through the secondary turns and the load resistance R_L. The secondary current then creates the secondary magnetic potential along the core, thus completing the feedback loop. The system model is a flux nulling and detecting scheme where the loop gain of the system is proportional to the sum of the two gain blocks SN_s and $F(s)$. Low frequency gain is provided by the gain block $F(s)$ and high frequency gain is provided by the gain block SN_s. It is assumed that the flux in the core is maintained at a low level by the system and that over this range of flux levels the reluctance of the core remains constant.

Basic Relationships

Following are some mathematical relationships which can be derived from these models to describe the system. The first equation

$$\text{TOTAL MMF} = N_p I_p + N_s I_s = R \Phi \tag{4.1a}$$

describes the magnetic potential summing action of the transformer and the block diagram in Figure 4.2. Equation 4.1a states that the total magnetic potential around the core produces flux in the core which is proportional to the reluctance of the core. By mathematical manipulation Equation 4.1a can be written

$$\frac{\text{TOTAL MMF}}{R} = \frac{N_p I_p}{R} + \frac{N_s I_s}{R} = \Phi \tag{4.1b}$$

where the terms $\frac{N_p I_p}{R} + \frac{N_s I_s}{R}$ have the units of flux and can be defined as

$$\frac{N_p I_p}{R} = \phi_p \tag{4.2}$$

and

$$\frac{N_s I_s}{R} = \phi_s \qquad\qquad (4.3)$$

A description of the physical significance of the symbols ϕ_p and ϕ_s follows.

Note that the above mathematical manipulations are equivalent to separating the reluctance block in Figure 4.2 and moving it through the summing point as shown in Figure 4.3. In Figure 4.3
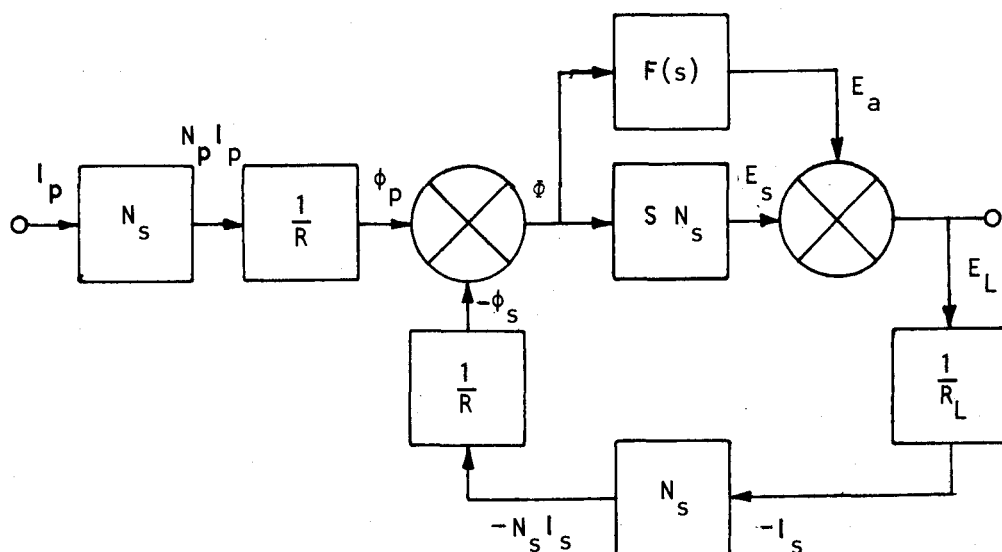
Figure 4.3. Modified Block Diagram of the Transformer

the total flux in the core Φ is now produced by the summation of two flux components represented by ϕ_p and ϕ_s. In this case ϕ_p represents a component of flux generated in the core by the primary magnetic potential and ϕ_s represents a component of flux generated in the core by the secondary magnetic potential. For ease of analysis, mention will be made of these two components of core flux. In this document

ϕ_p shall be known as "the primary generated flux" and ϕ_s shall be known as "the secondary generated flux".

Another equation

$$E_s = N_s \frac{d\phi}{dT} \qquad (4.4)$$

shows that E_s is the voltage generated in the secondary winding by the rate of change of flux in the core. Equation 4.4 expressed in terms of the Laplace variable S becomes

$$E_s(s) = N_s \, S \, \Phi(s) \; . \qquad (4.5)$$

The output of amplifier A_1 is generalized as a voltage source E_a. This source is related to the net core flux by the transfer function $F(s)$ as

$$E_a(s) = \Phi(s) \, F(s) \qquad (4.6)$$

where $F(s)$ has units of volts per Weber and represents the product of the flux to voltage transfer of the Hall device and the voltage gain of amplifier A_1 as a function of the Laplace variable S.

The last equation represents the algebraic sum of the voltages around the secondary circuit loop

$$E_L = -I_s \, R_L = E_s + E_a \qquad (4.7)$$

where E_L is the load or output voltage.

Some useful relationships can be derived from equations 4.1 through 4.7. One represents the net core flux relative to the primary generated flux which is derived in Appendix C as

$$\frac{\Phi}{\phi_p}(s) = \frac{1}{S \, T + 1 + \dfrac{T}{N_s} F(s)} \qquad (4.8)$$

where $T = \dfrac{L_s}{R_L}$ and is the transformer secondary time constant, and $\dfrac{\Phi}{\phi_p}$ is defined as the relative core flux. Another relationship repre-sents the ratio of output current to input current

$$\frac{I_s}{I_p} = \frac{N_p}{N_s} \left(\frac{\Phi}{\phi_p} - 1 \right) \qquad (4.9)$$

A third relationship shows that the input impedance of the system as a function of S is

$$Z_{in}(s) = \frac{E_p(s)}{I_p(s)} = \left(\frac{N_p}{N_s} \right)^2 S \frac{\Phi}{\phi_p}(s)\, L_s \qquad (4.10)$$

where $E_p(s)$ is the voltage across the primary turns as a function of S. The loop gain of the system is defined in terms of the primary and secondary generated flux as

$$G_L = \frac{-\phi_s}{\Phi} = \frac{1 - \dfrac{\Phi}{\phi_p}}{\dfrac{\Phi}{\phi_p}} \quad \cdot \qquad (4.11)$$

V.   ANALYSIS WITHOUT D.C. FEEDBACK

When F(s) equals zero the system operates as a normal transformer. In this case Equation 4.8 becomes

$$\frac{\Phi}{\Phi_p}(s) = \frac{1}{S\,T + 1} \qquad\qquad (5.1)$$

In Equation 5.1 as S approaches zero, the flux in the core equals the primary generated flux. For S values greater than $j\frac{1}{T}$, the net flux in the core is inversely proportional to S and approaches zero as S approaches infinity.

The loop gain from Equations 4.11 and 5.1 is

$$G_L = S\,T \qquad\qquad (5.2)$$

and when $S = j\frac{1}{T}$, the magnitude of the loop gain is unity. When Equations 4.9 and 5.1 are solved for the current transfer ratio, the result is

$$\frac{I_s}{I_p}(s) = \frac{N_p}{N_s}\ \frac{1}{S\,T + 1} \qquad\qquad (5.3)$$

Equation 5.3 illustrates the inability of the transformer to produce an output when S approaches zero. For S values greater than $j\frac{1}{T}$, however, the current transfer function approaches the transformer turns-ratio $\frac{N_p}{N_s}$. Figure 5.1, based upon Equations 5.1 and 5.3, shows the calculated curves of current transfer function and relative flux in the core versus frequency.

The input impedance as given by Equations 4.10 and 5.1 is

$$Z_{in}(s) = \left(\frac{N_p}{N_s}\right)^2 \frac{SL_s}{S\,T + 1} \qquad\qquad (5.4)$$

Figure 5.1

Frequency Response of Relative Core Flux
and Input to Output Ampere-turns Ratio
of the System without D.C. Feedback

— — Bode approx. of response
——— Calculated response
—·— Bode approx. of core flux response
         reduced by P. (chapt. 6)

$\dfrac{N_s I_s}{N_p I_p}$

$\dfrac{\Phi}{\Phi_p}$

Normalized Amplitude

Normalized Frequency, ωT

19
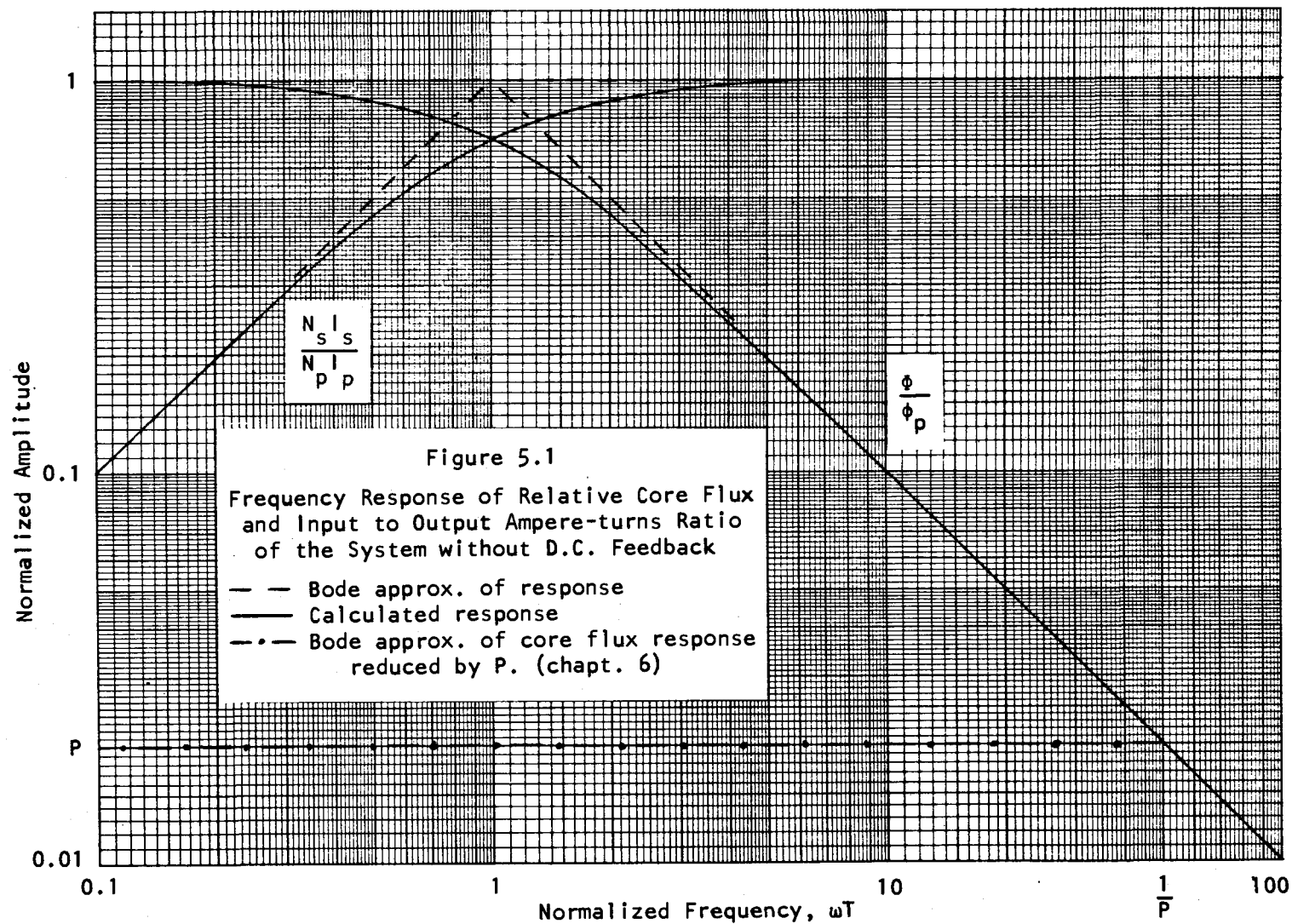
An equivalent circuit for the input impedance of the system under
discussion is shown in Figure 5.2.

Figure 5.2.   Input Impedance Equivalent Circuit

VI. ANALYSIS WITH D.C. FEEDBACK

In the system model a flux generated by the primary magnetic
potential is nulled at low frequencies by the Hall device and
amplifier A_1. The description of the transfer function of the Hall
device and amplifier A_1, with respect to S is given by the function
F(s). The value of F(s) will now be found which will reduce the
flux in the core to the ideal case where
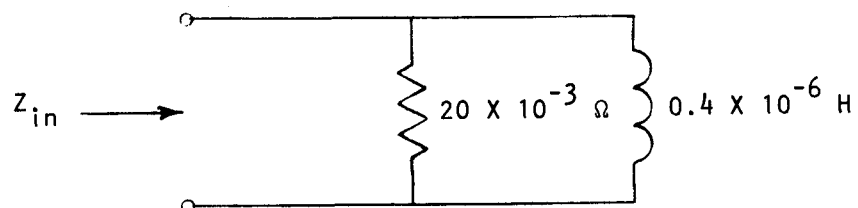
$$\frac{\Phi}{\phi_p}(s) = \frac{P}{1 + SPT} \qquad (6.1)$$

where P represents some fraction of the primary generated flux that
exists in the core when S equals zero. Equation 6.1 is based upon
Equation 5.1 when the low frequency flux is reduced by P and the
pole frequency of $\frac{\Phi}{\phi_p}(\omega)$ is extended by $\frac{1}{P}$. Note that in Figure 5.1
the slope of $\frac{\Phi}{\phi_p}(\omega)$ is one for frequencies above $\frac{1}{T}$ and that this is
the reason for extending the pole frequency the same amount as the
low frequency $\frac{\Phi}{\phi_p}$ is reduced.

Combining Equations 4.8 and 6.1 and solving for F(s) yields

$$F(s) = \frac{1-P}{P} \frac{N_s}{T} \qquad (6.2)$$

Equation 6.2 indicates that the response of F(s) for an ideal relative
core flux response is constant for all frequencies. A constant gain
for all frequencies is not feasible for a number of practical reasons
but Equation 6.2 does yield the desirable low frequency gain require-
ment for F(s).

When the bandwidth of amplifier A_1 is limited to the frequency

$\frac{1}{T_1}$, then the transfer function $F(s)$ has one pole at S equal to $\frac{1}{T_1}$.

If $\frac{1}{T_1}$ is related to T by

$$K = \frac{T_1}{T} \tag{6.3}$$

then

$$F(s) = \frac{1-P}{P} \frac{N_s}{T} \frac{1}{1 + SKT} \tag{6.4}$$

In this analysis all frequencies are normalized to the pole frequency of the transformer secondary. The term $\frac{1}{K}$ then is the pole frequency of the function $F(s)$ normalized to the transformer secondary pole frequency.

The core flux relationship resulting from Equations 4.8 and 6.4 is

$$\frac{\Phi}{\phi_p}(s) = \frac{P(1 + SKT)}{1 + S\{(K+1)TP\} + S^2 PKT^2} \tag{6.5}$$

which can be expressed in the form

$$\frac{\Phi}{\phi_p}(s) = \frac{P(1 + SKT)}{1 + 2\delta TS + S^2 T^2} \tag{6.6}$$

when δ is defined as the damping factor and T is the inverse of the pole pair frequency. These two equations are general and apply to the model over the complete frequency range. Two expressions, which are based upon Equations 6.5 and 6.6 are the frequency of the poles

$$\omega_p = \frac{1}{T} = \left(\frac{1}{KT^2 P}\right)^{\frac{1}{2}} \tag{6.7}$$

and the damping factor of the poles, which is defined as

$$\delta_p = \frac{K+1}{2} \left(\frac{P}{K}\right)^{\frac{1}{2}} \tag{6.8}$$
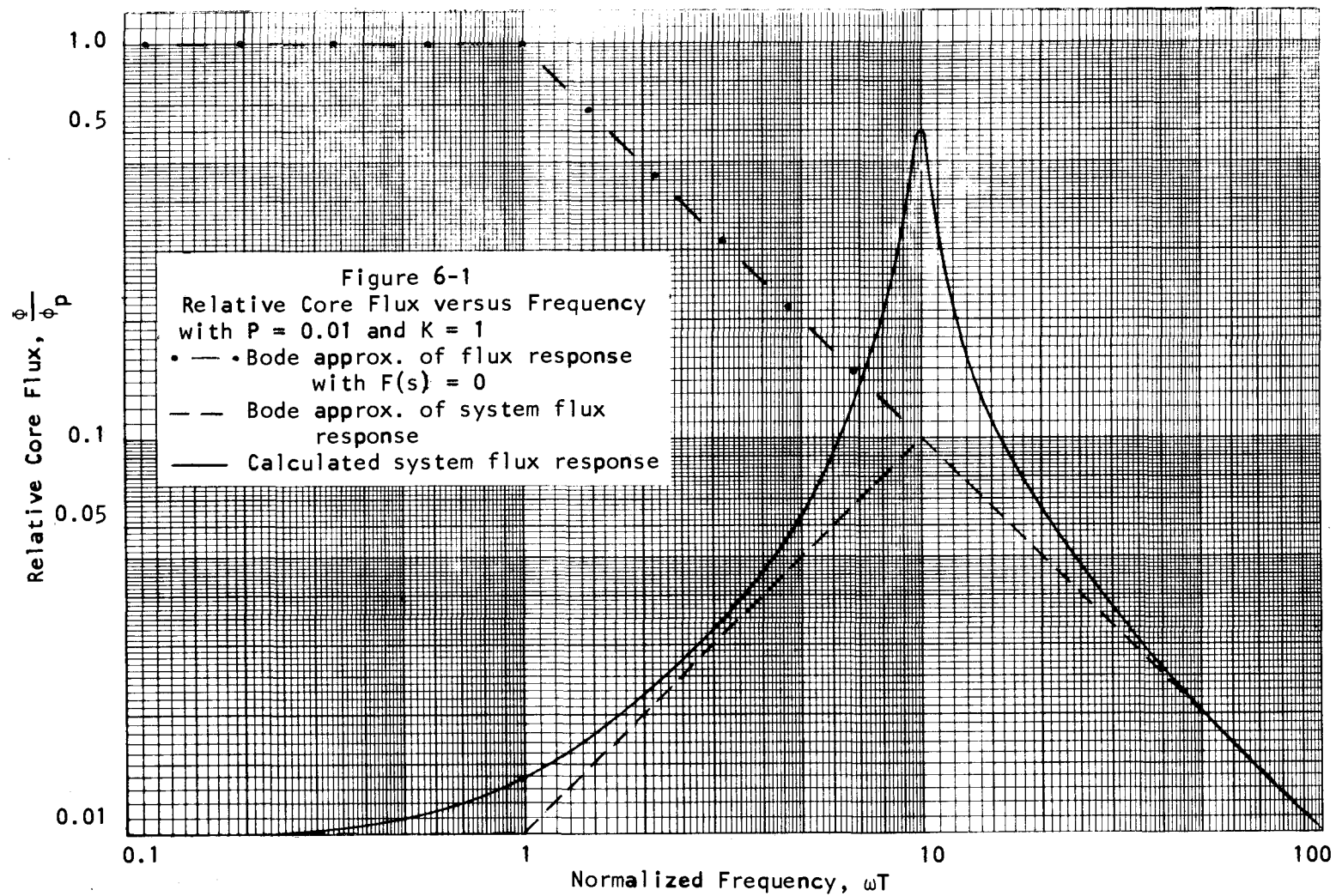
Core Flux

It was shown in Chapter IV that the relative core flux function is the basis for other parameters of the system such as the current transfer ratio and the system input impedance. The relative core flux function will also give an indication of the validity of the "core reluctance is constant" assumption. For instance, if the core flux becomes large at any frequency then the permeability of the core material will change and the assumption no longer holds. For these reasons the relative core flux function $\frac{\Phi}{\phi_p}$ (s) is analyzed.

Figure 6.1 is based upon Equations 6.5 and 6.6 and shows the Bode approximation as well as the calculated values for the relative core flux versus frequency for P equal to 0.01 and K equal to one. The pole frequency may be found graphically from Figure 6.1 at the crossover of the Bode approximation of the flux available from the effect of the transformer secondary turns, as plotted in Figure 5.1, and the Bode approximation of the flux reduction due to the transfer function F(s). The damping factor δ of this example is equal to 0.10. The overshoot resulting from the complex pole pair with this damping factor is shown by the solid line. (12:351) The maximum flux occurs at, or very near to, the pole frequency. An expression for the maximum relative core flux is found by substituting

$$S = j\frac{1}{T} \qquad\qquad (6.9)$$

into Equation 6.6 to obtain

$$\frac{\Phi}{\phi_p}(max) = \frac{P(1 + jK\omega_p)}{j2\delta_p} \qquad\qquad (6.10)$$

Figure 6-1
Relative Core Flux versus Frequency
with P = 0.01 and K = 1
•—•Bode approx. of flux response
with F(s) = 0
— — Bode approx. of system flux
response
——— Calculated system flux response

Relative Core Flux, $\frac{\Phi}{\phi_p}$

Normalized Frequency, ωT

The magnitude of the maximum relative core flux is
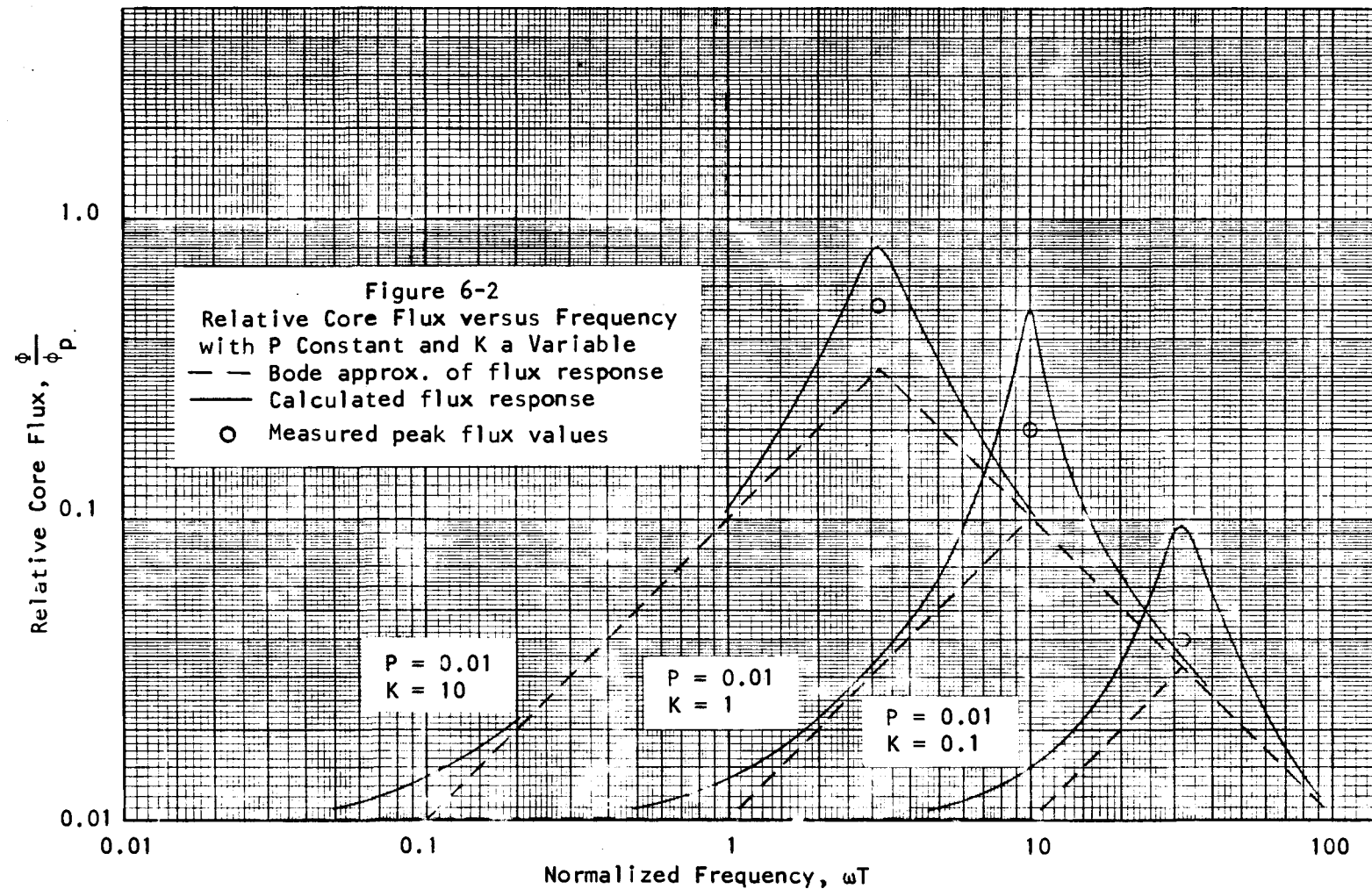
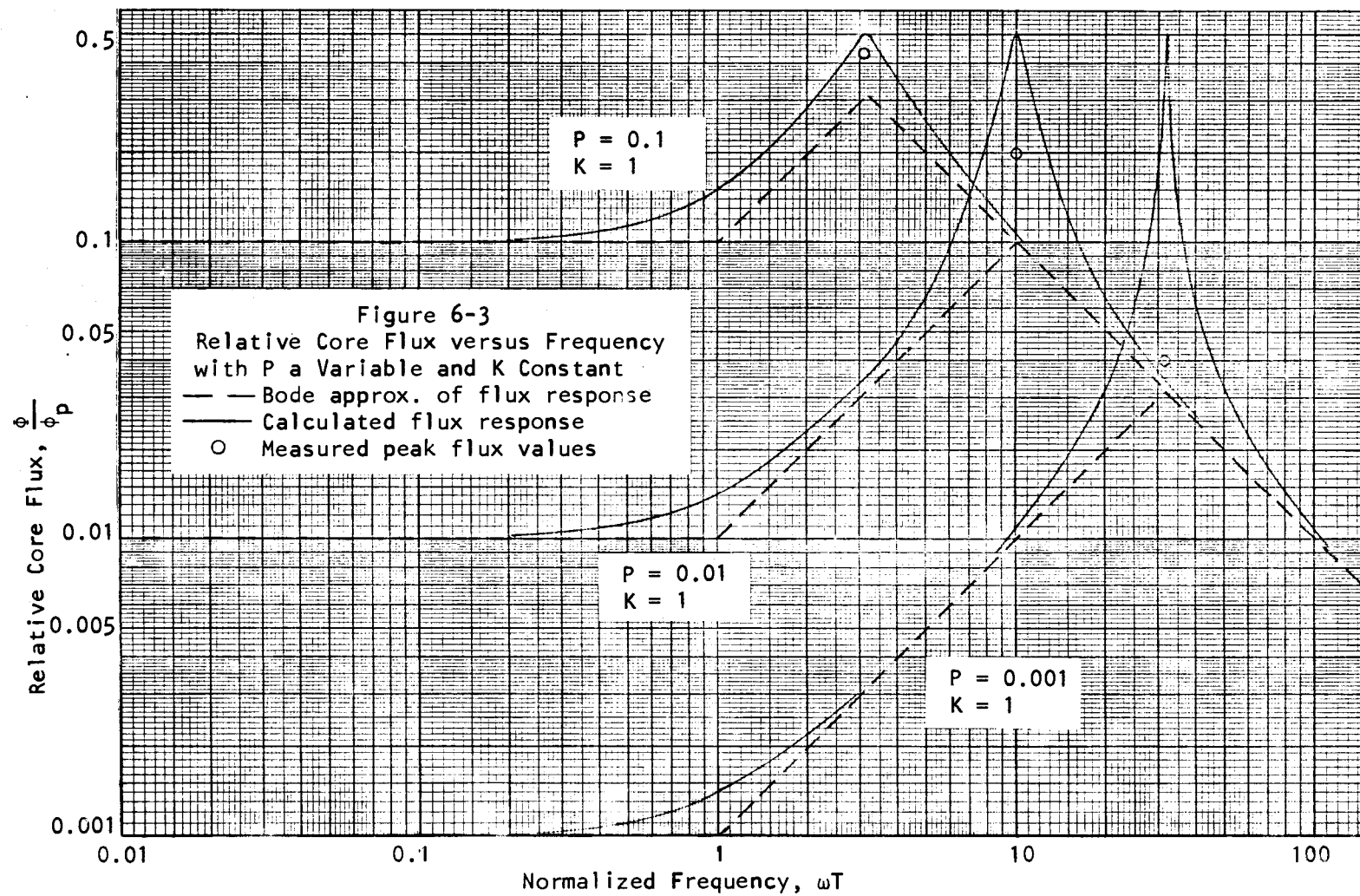$$\left|\frac{\Phi}{\phi_p}\right| (\text{max}) = \frac{K}{K+1} \left(1 + \frac{P}{K}\right)^{\frac{1}{2}} \qquad (6.11)$$

when ω_p and δ_p are defined by Equations 6.7 and 6.8.

Figures 6.2, 6.3 and 6.4 graphically illustrate the effects of K and P upon the relative core flux in the transformer model. Note again that the bandwidth or pole frequency of amplifier A_1 and F(s) is proportional to $\frac{1}{K}$ and that the gain of amplifier A_1 is proportional to $\frac{1}{P}$ when P is small; P is considered small when it is less that $\frac{1}{10}$. Figure 6.2 shows that the maximum relative core flux is reduced when the bandwidth of amplifier A_1 is increased. Figure 6.3 shows that changing the gain of amplifier A_1 does not reduce the maximum relative core flux. The only effect of increasing gain is a reduced damping factor. Figure 6.4 shows the effects on the maximum relative core flux if the gain bandwidth product of amplifier A_1 is limited above its pole frequency. In this case both the gain and bandwidth of amplifier A_1 are varied and the product of gain and bandwidth is constant. The graph shows that reducing the gain of the amplifier and extending the pole frequency reduces the flux in the core at the pole frequency. For the conditions shown in Figure 6.4, a minimum flux in the core over the complete frequency range occurs when the gain of the amplifier is approximately 10 and when K is approximately 0.1.

Current Transfer Function

The current transfer ratio is important because the system is

Figure 6-2
Relative Core Flux versus Frequency
with P Constant and K a Variable
— — Bode approx. of flux response
——— Calculated flux response
O Measured peak flux values

P = 0.01
K = 10

P = 0.01
K = 1

P = 0.01
K = 0.1

Relative Core Flux, $\frac{\Phi}{\Phi_P}$

Normalized Frequency, ωT

Figure 6-3
Relative Core Flux versus Frequency
with P a Variable and K Constant
— — Bode approx. of flux response
——— Calculated flux response
O   Measured peak flux values

P = 0.1
K = 1

P = 0.01
K = 1

P = 0.001
K = 1

Relative Core Flux, $\frac{\Phi}{\Phi_P}$

Normalized Frequency, ωT

27

Figure 6-4
Relative Core Flux versus Frequency
with the product PK constant
— — Bode approx. of flux response
——— Calculated flux response
O Measured peak flux values

P = 0.1
K = 0.1

P = 0.01
K = 1

P = 0.001
K = 10

Relative Core Flux, $\frac{\phi}{\phi_p}$

Normalized Frequency, ωT

28

to be used as a current measuring instrument. When the system is
ideal, the secondary current is equal to the primary current times
the turns-ratio at all frequencies. Deviations or aberrations from
the ideal performance are important in that they should be minimized.

From Equation 4.9 the ampere-turns transfer from the primary to
secondary is

$$\frac{N_s I_s}{N_p I_p} = \frac{\Phi}{\phi_p} - 1 \tag{6.12}$$

When the percent aberrations in the current transfer characteristic
is defined as

$$\% \text{ Aberrations} = \frac{N_p I_p - N_s(-I_s)}{N_p I_p} \times 100 \tag{6.13}$$

then

$$\% \text{ Aberrations} = \frac{\Phi}{\phi_p} \times 100 \tag{6.14}$$

and figures 4.4 through 4.7 can represent the aberrations of the
current transfer function normalized to 100%. Thus if

$$\frac{\Phi}{\phi_p} \ll 1 \tag{6.15}$$

no aberrations exist in the current amplitude response and the
ampere-turns of primary magnetic potential essentially equals the
ampere-turns of secondary magnetic potential. However, the current
amplitude response has a 50% aberration at the pole frequency if

$$\frac{\Phi}{\phi_p}(\text{max}) = 0.5 \tag{6.16}$$

Input Impedance

The input impedance or insertion impedance of this system is important in its effect upon the circuit being tested. As a current measuring instrument, it should have a very low input impedance at all frequencies. Further, the impedance should be well-defined and not change abruptly at any frequency. The input impedance of the system was found in Equation 4.10 which is

$$Z_{in}(s) = \left(\frac{N_p}{N_s}\right)^2 L_s \, S \, \frac{\Phi}{\phi_p}(s) \qquad (4.10)$$

which contains the term $S \frac{\Phi}{\phi_p}(s)$. This term represents the time derivative of the relative core flux when S is the Laplace transform of $\frac{d}{dT}$. The result of this term is to add a 20 db/decade slope to all points of the relative core flux curves. Therefore, when $\frac{\Phi}{\phi_p}(\omega)$ is constant the input impedance is inductive. When $\frac{\Phi}{\phi_p}(\omega)$ decreases with frequency, the input impedance is resistive. The peak that occurs in the $\frac{\Phi}{\phi_p}(\omega)$ response also occurs in the input impedance response.

The general relationship for the input impedance is found from Equation 4.10 and the relative core flux relationship, Equation 6.5. The result is

$$Z_{in}(s) = \left(\frac{N_p}{N_s}\right)^2 L_s \, S \, \frac{P(1 + SKT)}{1 + S\{(K+1)TP\} + S^2 PKT^2} \quad . \qquad (6.17)$$

Figure 6.5 shows the frequency response of the input impedance given by Equation 6.17 when P = 0.01 and K = 1. The low frequency imped-ance from Equation 6.17 is

Figure 6.5
Input Impedance versus Frequency
with P = 0.01 and K = 1
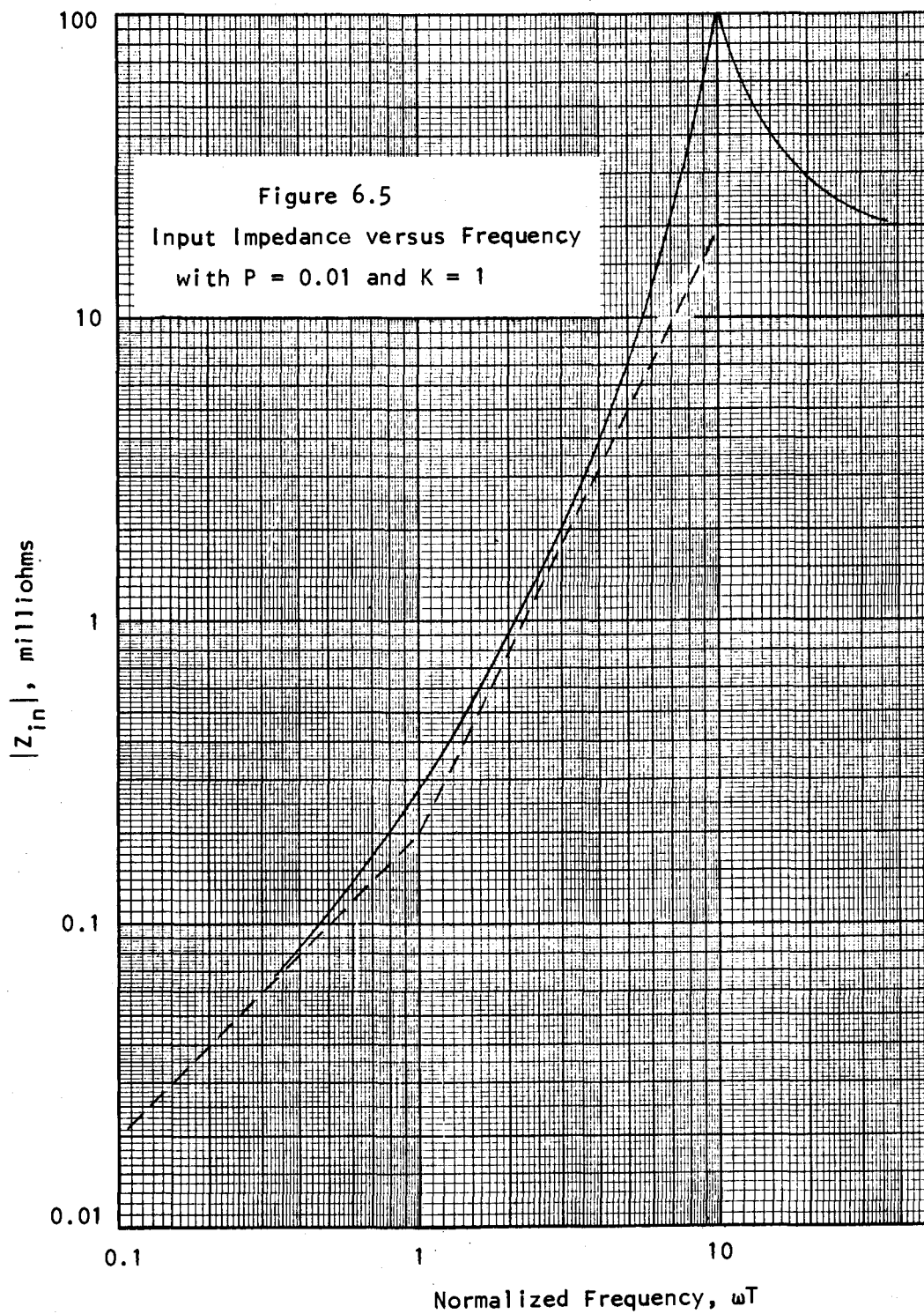
$$Z_{in}(S \to 0) = \left(\frac{N_p}{N_s} \right)^2 P\ S\ L_s \quad . \tag{6.18}$$

The low frequency inductance can be found from Equation 6.18 when $\frac{N_p}{N_s} = \frac{1}{50}$; $L_s = 1 \times 10^{-3} H$; $P = 0.01$ and $K - 1.0$ and is

$$L_{in} = \left(\frac{N_p}{N_s} \right)^2 P\ L_s = 4 \times 10^{-9} \text{ Henrys.} \tag{6.19}$$

At high frequencies the input impedance is

$$Z_{in}(S \to \infty) = \left(\frac{N_p}{N_s} \right)^2 R_L = 20 \times 10^{-3} \text{ ohm} \tag{6.20}$$

when $T = \frac{s}{R_L}$.

The optimum input impedance response in the midfrequency range is obtained when the relative core flux response has no peak at the pole frequency.

System Stability

It can be shown that the denominator of the current transfer function, Equation 6.12, is Hurwitz. Therefore, the poles of the transfer function can never occur in the right half of the S plane and the stability of the system as described by this model is maintained. Pole locations do exist very close to the $j\omega$ axis of the S plane for some values of gain and bandwidth of amplifier A_1. This is substantiated by the low damping factor apparent in some of the plots of Figures 6.1, 6.2, 6.3 and 6.4. If any additional high frequency poles are involved under these conditions, the system could, with sufficient

loop gain, become unstable.

Theoretical Conclusions

It has been shown that the current and input impedance responses are based upon the response of the relative core flux. When the relative core flux response has no peak, the input impedance becomes a simple parallel inductance and resistance. When the response of the relative core flux remains below 0.01, the current transfer response has less than 1% aberrations. Some requirements for an optimum core flux response based upon the investigation thus far are; (1) the best performance is obtained when the bandwidth of the function $F(\omega)$ is infinite and the loop gain is greater than 100; (2) when the bandwidth of the function $F(\omega)$ cannot be infinite, it should be as high as possible to reduce $\frac{\Phi}{\phi_p}(\max)$; (3) increasing the loop gain of the system model does not reduce $\frac{\Phi}{\phi_p}(\max)$ and does not reduce aberrations in the current transfer response or the input impedance response.

VII.   EXPERIMENTAL RESULTS

The system which is described was built and tested throughout the frequency range of interest. The transformer core was tested to determine the amount of flux which can be contained in the core without distortion. Experimental results showed that the flux established in the core by 0.5 ampere-turns of total magnetic potential caused an allowable distortion of 2% in the core characteristics. The net core flux should not exceed the 0.5 ampere-turn level when the input magnetic potential is equal to the maximum rated 10 ampere-turns. This requires that

$$\frac{\Phi}{\Phi_p} < 0.05 \qquad\qquad (7.1)$$

for all frequencies.

The available loop gain of the system was measured when the gain and bandwidth of the amplifier were not limited. The available loop gain response is shown in Figure 7.1. The zero of the response at approximately 60 KHz is attributed to the zero in the Hall device response as shown in Figure 3.1. Multiple poles occur in the loop gain response above one megahertz. One pole is attributed to the input capacitance of amplifier A_1 and the output resistance of the Hall device. Other poles are attributed to the integrated circuit linear amplifier which forms part of amplifier A_1. The specified gain bandwidth product of this circuit is 400 KHz. The net result of these multiple poles is that the loop gain of the system must equal unity at, or near, 5 MHz because the rate of decreasing gain approaches

Figure 7.1
Available Loop Gain versus Frequency
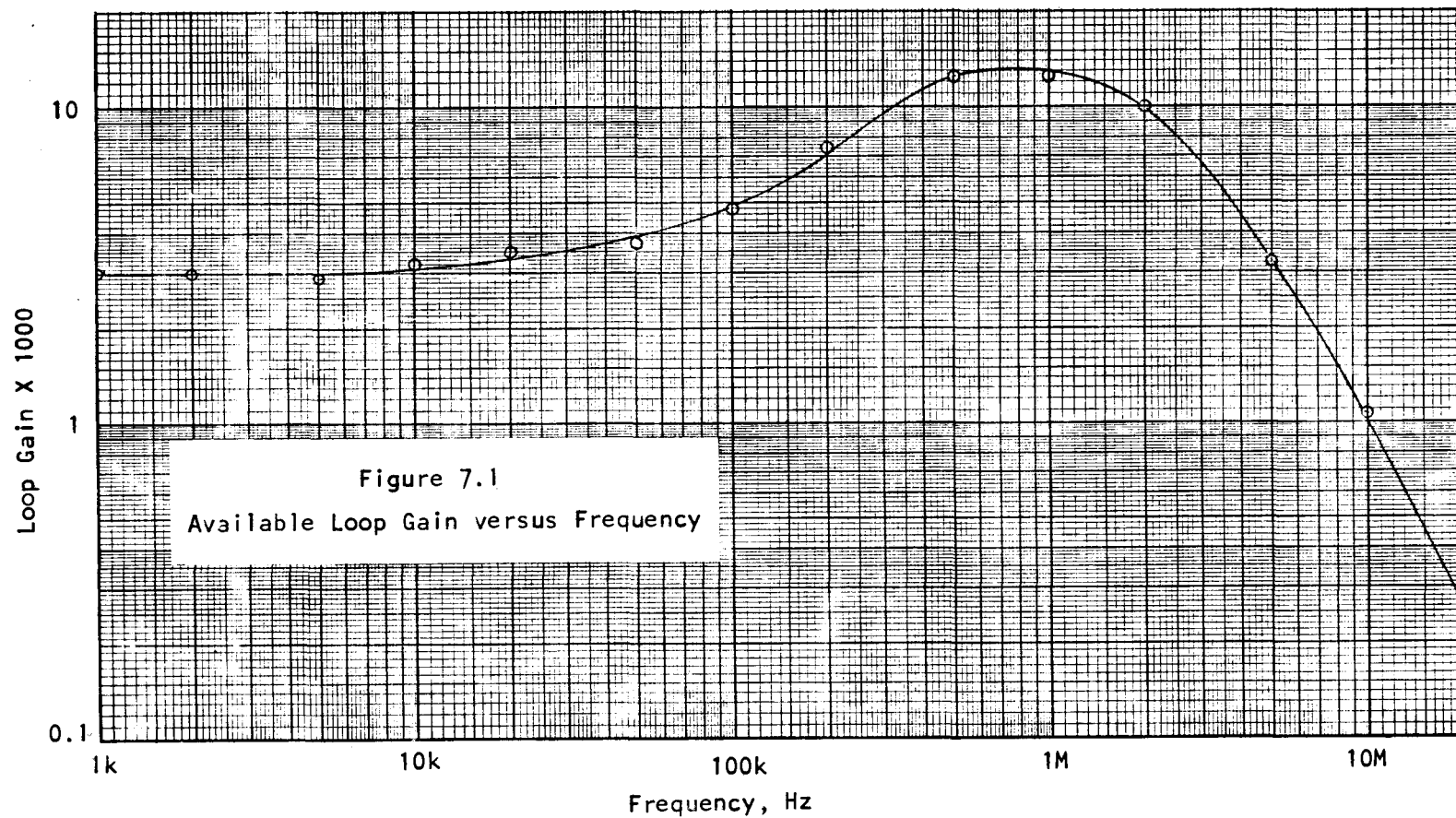
40 db/decade and the phase shift of the loop gain approaches 180 degrees at that frequency. (12:353)

Adjustments were provided in amplifier A_1 to vary the gain and the lowest pole frequency of the amplifier response. The data in Table I was obtained when the loop gain and the amplifier pole frequency were selected as indicated by the values of P and K. The values and frequencies of the peak flux were calculated from the data in Table I by using Equation 4.9 which is

$$\frac{I_s}{I_p} = \frac{N_p}{N_s} \left(\frac{\Phi}{\phi_p} - 1 \right) \qquad (4.9)$$

The pole frequency of the transformer secondary circuit $\frac{1}{2\pi T}$ was found to be 6 KHz and the data in Table I must be normalized to this frequency to correlate with the graphs in section six.
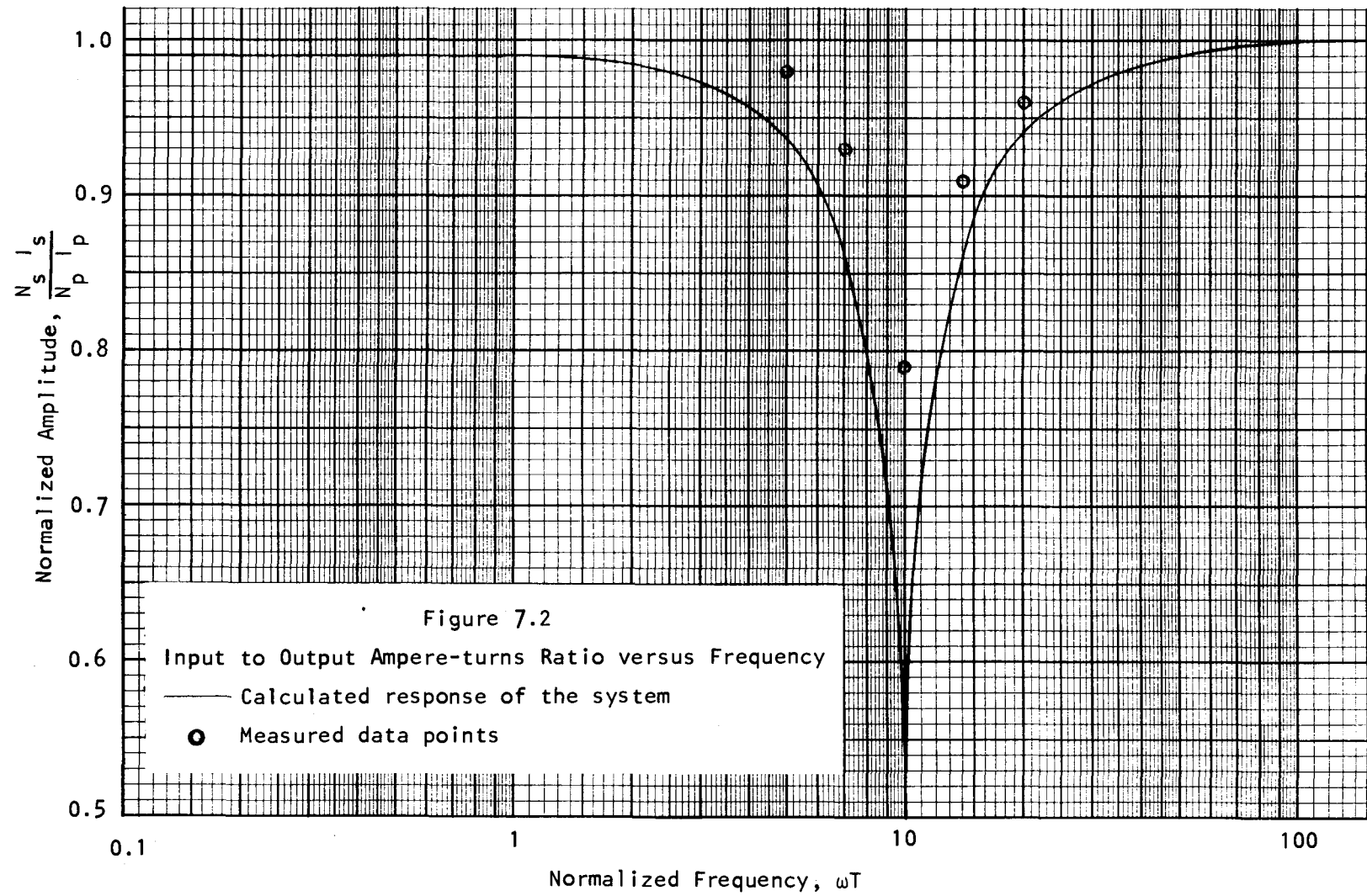
Some comparison of the results in Table I with the calculated results is indicated. The pole frequency as determined by Equation 6.7 and the measured frequency of minimum current output correlated very well. The magnitude of the aberrations in the measured response were significantly smaller than the calculated aberrations. Illustrating this point, Figure 7.2 represents the calculated as well as the measured ampere-turns response of the system when P equals 0.01 and K equals one. Figure 6.1 showed the theoretical flux response under these same conditions. The calculated peak flux in the core, from Figure 6.1, is 0.5 ϕ_p while the measured peak flux value, calculated from Table I, is 0.2 ϕ_p. The reason for the smaller measured aberrations and the lower peak flux points may be explained by the existence of losses and stray components which are not

TABLE I

Amplitude versus Frequency Data for Varying Values of P and K

P = 0.1 K = 0.1		P = 0.1 K = 1		P = 0.1 K = 10	
Frequency KHz	$\frac{N_s I_s}{N_p I_p}$	Frequency KHz	$\frac{N_s I_s}{N_p I_p}$	Frequency KHz	$\frac{N_s I_s}{N_p I_p}$
30	0.90	9.5	0.85	3	0.72
42	0.90	13.3	0.74	4.2	0.32
60	0.90	*18	0.57	*6	0.12
85	0.94	26.5	0.80	8.5	0.50
120	0.96	38	0.94	12	0.80

P = 0.01 K = 0.1		P = 0.01 K = 1		P = 0.01 K = 10	
Frequency KHz	$\frac{N_s I_s}{N_p I_p}$	Frequency KHz	$\frac{N_s I_s}{N_p I_p}$	Frequency KHz	$\frac{N_s I_s}{N_p I_p}$
95	0.98	30	0.98	9.5	0.95
132	0.97	42	0.93	13.2	0.85
*190	0.96	*62	0.80	*19	0.48
265	0.96	85	0.91	26.5	0.81
380	0.98	120	0.96	38	0.93

P = 0.001 K = 0.1		P = 0.001 K = 1		P = 0.001 K = 10	
Frequency KHz	$\frac{N_s I_s}{N_p I_p}$	Frequency KHz	$\frac{N_s I_s}{N_p I_p}$	Frequency KHz	$\frac{N_s I_s}{N_p I_p}$
300	∞	95	1.00	30	0.98
420	∞	135	0.98	42	0.95
600	∞	*200	0.96	*60	0.78
850	∞	265	0.97	85	0.90
1200	∞	380	0.98	120	0.96

* Indicates the frequency at which the minimum output current

was measured.

Figure 7.2

Input to Output Ampere-turns Ratio versus Frequency

——— Calculated response of the system

⊙   Measured data points

included in the system model.

The result of the damping factor limitation alters the conclusions based upon the theoretical results. Figure 6.3 shows that increasing loop gain should have little affect upon the peak flux in the core. However, when the damping factor is limited, the flux in the core is reduced when gain is increased as shown by the three maximum flux points calculated from the data in Table I by using Equation 4.9.

The best ampere-turn response is obtained when the gain-bandwidth product of amplifier A_1 is optimized for a maximum stable value. Table I shows an amplitude response aberration of 4% either when P equals 0.01 and K equals 0.1 or when P equals 0.001 and K equals one. When the loop gain-bandwidth product was increased to 60 MHz, P equaled 0.001 and K equaled 0.1, the system was unstable verifying the loop gain-bandwidth limitation.

The input impedance of the system could not be measured with any accuracy for two reasons. One reason is that the length of wire necessary for the primary turn to pass through the transformer core has more inductance than the system as calculated in Equation 6.21. (7) The other reason is that the transformer core assembly is shielded from external magnetic fields by a case of high permeability material. This case also creates an appreciable impedance in the primary turn. Peaks can be detected in the frequency response of the voltage across the primary turn. These peaks did occur at the relative flux pole frequencies even though their relative magnitude could not be determined accurately.

VIII.   CONCLUSIONS

The current measuring system which is described is a practical device with aberrations smaller than 4%. There is, however, an unavoidable peak in the flux response and adjustments are necessary to force the peak relative core flux value to less than 0.04. The major limitation causing this response problem is the gain-bandwidth product limit imposed by the high frequency poles in amplifier A_1. The next step in improving the system performance is to eliminate these poles or to push them to higher frequencies. Other effects such as the secondary winding capacitance and the delay of the probe cable might then limit the loop gain-bandwidth product. Enough bandwidth might be gained to eliminate the peak in the relative flux response.

The signal flow approach to the analysis of this system has been particularly suitable and might be applicable to other transformer systems which operate over a broad frequency range. It is seen that the null signal in the system is the flux in the core and therefore is the focal point of the system analysis. Other parameters of the system are easily derived from the relative core flux.

This model can be readily extended to include more stray components such as leakage flux, secondary winding capacitance and higher frequency poles in amplifier A_1 among others. The same basic analysis technique can be used. The results, however, become more esoteric when this is done and care must be taken to maintain meaning in the analysis results.

In conclusion, it is noted that the use of this system need not be limited to current measurements. Magnetic fields can be measured accurately by opening the magnetic circuit. In this case the Hall device could be installed in the center of what is now the secondary winding. Magnetic flux passing through the Hall device and coil would be detected and then nulled by the current through the winding. This current would then be proportional to the magnetic flux passing through the coil opening.

BIBLIOGRAPHY

1. Dunlap, W. Crawford. An introduction to semiconductors. New York, Wiley, 1957. 417p.

2. Corcoran, George F. and Henry R. Reed. Introductory electrical engineering. New York, Wiley, 1957. 527p.

3. Engle, J. F. and H. J. Oorthuys. Introductory notes to electric and magnetic fields. Corvallis, Oregon State College Cooperative Association, 1959. 84p.

4. Hall, H. E. On a new action of the magnet on electric circuits. American Journal of Mathematics, 2:287. 1879.

5. Heartz, Robert A. and Herbert Buelteman Jr. The application of perpendicularly superimposed magnetic fields. American Institute of Electrical Engineers Transactions, 74:655-660. Nov. 1955.

6. Holl, Dio L.; Clair G. Maple and Bernard Vinograde. Introduction to the Laplace transform. New York, Appelton, 1959. 174p.

7. Lee, Lawrence E. Rapid selection of vhf bypass capacitors. Electronics, Dec. 28, 1962, p44-46.

8. Lindmayer, Joseph and Charles Y. Wrigley. Fundamentals of semiconductor devices. Princeton, Van Nostrand, 1965. 486p.

9. Plonsey, Robert and Robert E. Collin. Principles and applications of electromagnetic fields. New York, McGraw, 1961. 554p.

10. Ryder John D. Networks, lines and fields. 2d ed. Englewood Cliffs, Prentice-Hall, 1955. 593p.

11. Van Valkenburg, M. E. Introduction to modern network synthesis. New York, Wiley, 1964. 498p.

12. Westman, H. P. et al. Reference data for radio engineers. 4th ed. New York, International Telephone and Telegraph Corporation, 1965. 1121p.

APPENDICES

APPENDIX A

A List of Symbols

A_h Hall device area

B magnetic flux density

E_a output voltage of amplifier A_1

E_{he} Hall effect voltage

E_n Hall device ½ turn voltage

E_s transformer secondary voltage

E_p transformer primary voltage

F transfer function from flux to voltage of the Hall device and amplifier A_1.

G_L system loop gain

I_h Hall device current

I_p transformer primary current

I_s transformer secondary current

K pole time-constant of amplifier A_1 normalized to the pole time-constant of the transformer secondary

L_s inductance of the secondary turns

N_h the turn of the Hall device output leads

N_p transformer primary turns

N_s transformer secondary turns

P low frequency ratio of net core flux to primary generated flux

R reluctance

R_h Hall coefficient

R_L the load resistance in series with the transformer secondary turns

S   the Laplace variable representing complex frequency

T   the transformer secondary time-constant

T_1 amplifier A_1 pole time-constant

T_h Hall device thickness

Z_{in} system input impedance or insertion impedance

δ damping factor

Φ net core flux or total core flux

ϕ_p primary generated flux; flux component generated in the core

     by the primary magnetic potential

ϕ_s secondary generated flux; flux component generated in the core

     by the secondary magnetic potential

ω_o frequency of zero

ω_p frequency of pole

APPENDIX B

Proof that Reluctance Equals Turns^2 Over Inductance

The magnetic circuit relationship is

$$\Phi = \frac{N\ I}{R} \tag{b.1}$$

where Φ is the amount of flux in Webers in the flux path, N is the number of turns linking the flux path, I is the current through the turns in amperes, and R is the reluctance to flux along the path in ampere-turns per Weber. The potential induced in the turns if the magnetic field is changing is

$$E = N \int \frac{dB}{dT} \cdot dA \tag{b.2}$$

where B is the flux density in Webers per meter^2 passing through the area A which is in meter^2.(2:3-34) The time variable is represented by T in seconds. In a transformer where the flux is normal to the windings and bounded by the transformer core, Equation b.2 becomes

$$E = N\ A\ \frac{dB}{dT} = N\ \frac{d\Phi}{dT} \tag{b.3}$$

and if combined with Equation b.1 is

$$E = \frac{N^2}{R}\ \frac{dI}{dT} \tag{b.4}$$

The inductance of the turns can be defined as

$$L = \frac{1}{E}\ \frac{dI}{dT} \tag{b.5}$$

where L is the inductance in Henrys. When Equation b.5 is combined with Equation b.4 the result is

$$L = \frac{1}{E} \frac{dI}{dT} = \frac{N^2}{R}$$ (b.6)

and solving for reluctance

$$L = \frac{N^2}{R}$$ (b.7)

The reluctance of the flux path in a transformer is found by measuring the inductance of a winding and dividing this value into the square of the number of turns of the winding.

and when I_s is substituted into Equation c.4 the result is

$$\Phi(s) = \frac{-(\Phi(s) - \phi_p(s)) N_s R_L}{(F(s) + SN_s) L_s} \quad . \qquad (c.9)$$

Solving for relative core flux, $\frac{\Phi}{\phi_p}(s)$ gives

$$\frac{\Phi}{\phi_p}(s) = \frac{1}{S\dfrac{L_s}{R_L} + 1 + \dfrac{L_s}{R_L N_s}F(s)} \qquad (c.10)$$

and when $T = \dfrac{L_s}{R_L}$ Equation c.10 becomes

$$\frac{\Phi}{\phi_p} = \frac{1}{ST + 1 + \dfrac{T}{N_s}F(s)} \qquad (c.11)$$

which is equivalent to Equation 4.8 in Chapter IV.